Pure Appl. Chem., Vol. 83, No. 1, pp. 43–55, 2011.
doi:10.1351/PAC-CON-10-11-02

Conjugated polyelectrolyte–lipid interactions: Opportunities in biosensing*

An Thien Ngo, Pierre Karam, and Gonzalo Cosa‡

Department of Chemistry and Center for Self-Assembled Chemical Structures, McGill University, 801 Sherbrooke Street West, Montreal, QC H3A 2K6, Canada

Abstract: Fluorescent conjugated polyelectrolytes (CPEs) have attracted considerable interest over the past decade as novel materials for developing biosensing schemes and sensing devices for biomolecules. This interest stems from the exquisite polymer sensitivity to the presence of fluorescence quenchers, enabling amplified sensing of molecules of interest. Efficient energy transport along the polymer backbone is critical to their sensing capabilities. Considerable research efforts have thus gone into understanding and controlling energy transport along the polymer backbone. In particular, it has been shown that interactions between CPEs with either surfactants or lipid molecules may significantly reduce energy transport along the polymer backbone that in turn may provide for unique biosensing opportunities. In the first half of this review, we give a historical overview on energy transport in conjugated polymers and polyelectrolytes. In the second half, we summarize the most recent work on the interaction of CPEs with surfactants with an emphasis on our own work elucidating electronic energy transport in CPEs encapsulated into lipid vesicles or embedded within the membrane of lipid vesicles.

Keywords: analytical chemistry; fluorescence; imaging; materials; nanoparticles.

CONJUGATED POLYMERS AND CONJUGATED POLYELECTROLYTES

Conjugated polymers are organic macromolecules with a backbone of alternating single and double bonds functionalized with side-groups to facilitate their solubility. They are characterized by their high emission quantum yield, large molecular weight, and the rapid transport of charge carriers and excitons along the π-conjugated backbone [1–3]. Given their unique properties, these novel materials hold great promise as building blocks in the construction of optoelectronic devices (i.e., electroluminescent, photovoltaic, and sensor devices) [4].

Among a number of different conjugated polymers prepared and characterized over the past three decades, the conjugated polymer poly(*p*-phenylenevinylene) (PPV, Fig. 1) attracted enormous attention early on owing to its high luminescence properties. This polymer was the first one utilized in preparing electroluminescent devices [5], and while organic light-emitting diodes (LEDs) had been fabricated in the 1980s using small molecules such as anthracene [6], a polymer-based LED allowed the field of organic electronics to take shape. A major limitation to the use of PPV (and conjugated polymers in general) was, however, its poor solubility, which led to intense research into functionalizing the polymer backbone with alkyl groups in order to increase their solubility and processing ability in organic

Pure Appl. Chem. **83**, 1–252 (2011). A collection of invited, peer-reviewed articles by former winners of the IUPAC Prize for Young Chemists, in celebration of the International Year of Chemistry 2011.
‡Corresponding author: E-mail: gonzalo.cosa@mcgill.ca

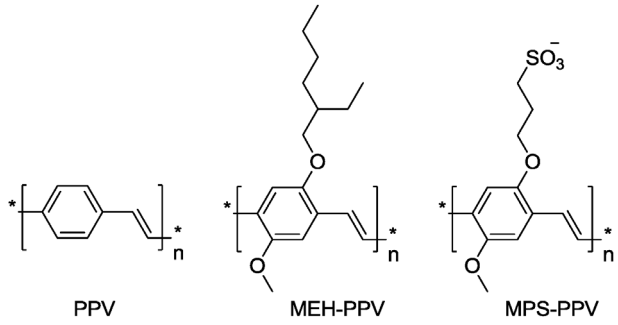

Fig. 1 Structures of the conjugated polymers poly(*p*-phenylene vinylene) (PPV), poly[2-methoxy, 5-(2'-ethyl-hexyloxy)-*p*-phenylene vinylene] (MEH-PPV) and poly(5-methoxy-2-[3-sulfopropoxy)-*p*-phenylene vinylene] (MPS-PPV).

solvents. A number of PPV-related polymers with different substitution patterns were thus prepared, and their synthesis and spectroscopic characteristics were recently reviewed [7,8].

More recently, the functionalization of conjugated polymers with ionic groups, such as alkyl-sulfonate groups, led to the development of conjugated polyelectrolytes (CPEs). A 3-(4-sulfonatobutyl)-substituted polythiophene was first reported in 1987, opening opportunities to manipulate and exploit the polymer properties using water as a solvent [9]. In 1990, Wudl reported on the first water-soluble CPE bearing a PPV backbone, poly[5-methoxy-2-(3-sulfopropoxy)-*p*-phenylene vinylene] (MPS-PPV, see Fig. 1) [10]. Recent reviews discuss the preparation, photophysics, and applications of CPEs [1,11].

EXCITON MIGRATION IN CONJUGATED POLYMERS

The unique opportunities that conjugated polymers provide for developing novel optoelectronic materials have triggered a number of research efforts aimed at understanding electronic energy transfer or exciton migration in conjugated polymers. Ensemble and single-molecule spectroscopic studies have shown that polymer conformation plays a key role in modulating exciton transport. Rapid through-space exciton migration is normally encountered in polymer chains that are highly folded and/or aggregated, but it is not common in extended polymer chains, where through-bond energy transfer is the dominant exciton transport mechanism [12,13]. In the former case, energy is transferred between conjugated polymer chain segments via resonance energy transfer, where the oscillation of an excited transition dipole in a segment induces oscillations in appropriately oriented transition dipoles in adjacent segments [14–16]. Interchain energy transfer (through-space) is more efficient than intrachain energy transfer (through-bond).

Quantum-mechanical simulations and time-resolved fluorescence experiments estimate the time scale for through-bond energy transfer on the order of nanoseconds, while through-space energy transfer occurs in picoseconds [13,16]. An experiment by Schwartz and co-workers demonstrated the relative rate of the two mechanisms [12,17]. Individual conjugated polymer chains were confined within silica mesopores, such that a portion of the chain extended outside the pore. The assemblies were oriented such that the pores were vertical to the laboratory plane. When excited with horizontally polarized light, a rapid initial loss in emission anisotropy (horizontal) indicated fast energy transfer through-space among the randomly oriented segments external to the pores. A subsequent slower rise in emission anisotropy (vertical) indicated through-bond energy transfer from these randomly oriented segments to the vertically oriented polymer segments within the pores [12,17].

Single-molecule studies

Exciton migration was visualized at the single-molecule level for the first time in 1997 by Barbara and Swager [18]. A spun-cast film of poly(*p*-phenylene vinylene)-poly(*p*-pyridinylene vinylene) of molecular weight approximately 20 kDa (20 monomers) diluted in a nonfluorescent matrix of polystyrene, exhibited stepwise blinking (Fig. 2). The molecules alternated between three distinct levels of intensity, and photobleached in a single step. This indicated that the entire molecule, or large portions thereof, was behaving as a single chromophore unit. The authors attributed the blinking to reversible photochemical oxidation [19].

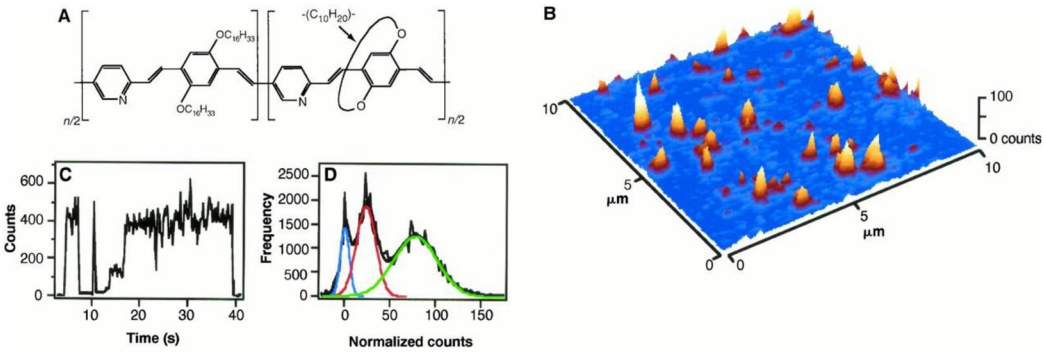

Fig. 2 Stepwise photobleaching of individual conjugated polymer molecules, demonstrating efficient exciton migration. (A) Poly(*p*-phenylene vinylene)-poly(*p*-pyridinylene vinylene) (PPV-PPyV). (B) Scanning confocal image of a spun-cast film of PPV-PPyV in polystyrene. Each spot corresponds to a single PPV-PPyV molecule. (C) Intensity-time transient of a single PPV-PPyV molecule. (D) Histogram showing three distinct levels of intensity exhibited by the individual molecules. From van den Bout et al. *Science* **277**, 1074 (1997). Reprinted with permission from the American Association for the Advancement of Science.

These studies were next extended to the widely used polymer poly[2-methoxy, 5-(2'-ethyl-hexyl-oxy)-*p*-phenylene vinylene] (MEH-PPV, Fig. 1). The polymer molecules, consisting of ~2000 repeat units, exhibited stepwise blinking behavior with discrete intensity levels [20]. The lower intensity level was attributed to a reversibly formed, photochemically generated, fluorescence quencher; while the higher level corresponded to its repair. A blue shift was also observed in the single-molecule spectra of MEH-PPV molecules upon extended irradiation. Barbara proposed a "funneling" model based on ensemble site-selective fluorescence studies, summarized in ref. [21], where the distribution in chromophore length, combined with the tendency of the excited state to perform a random walk throughout the polymer, would lead to the through-space intramolecular transfer of energy from higher-energy (shorter) chromophores to lower-energy (longer) chromophores. The blue shift upon extended irradiation of the polymer would then result because energy funneling to the lower-energy segments rendered them more prone to photochemical reactions generating fluorescence-quenching sites. The lower-energy sites would therefore be expected to photobleach first, producing a blue shift as emission would then preferentially arise from the higher-energy sites.

Shortly thereafter, Rothberg used single-molecule spectroscopy to elucidate why the fluorescence of spun-cast conjugated polymer films depended on the film processing conditions [22]. MEH-PPV is poorly solvated in toluene where it is largely aggregated but adopts a more extended conformation in the relatively more polar solvent chloroform; this has been demonstrated by light-scattering measurements in the ensemble [17]. Single-molecule intensity/time trajectories revealed that the solution conformation was preserved upon spin-casting. Thus, single MEH-PPV molecules exhibited stepwise photobleaching and blinking when spun-cast from toluene (where they remained largely aggregated),

and exponential photobleaching when spun-cast from chloroform (where extended polymer chains were presumably obtained) [22]. These experiments illustrated the difference in energy transfer rates through-space (fast) vs. through-bond (slow) and provided guidelines for the design of devices, where an extended conformation would be desirable for maximizing the quantum yield of electroluminescent devices while an aggregated conformation would optimize the function of sensor devices based on amplified fluorescence quenching [22].

Aggregation of the polymer, by increasing the degree of electronic coupling between adjacent chromophores [23], tends to increase the efficiency of energy transfer and favor the fast interchain mechanism [12,17]. As a result, more emission is seen from low-energy sites compared to higher-energy sites, producing a red shift in the fluorescence emission [24]. Aggregation furthermore reduces the polymer's fluorescence quantum yield, due to the increase in probability that the excited state will visit a nonemissive site [13] such as that caused upon photo-oxidation [20,25] or upon the formation of interchain species whose decay is nonradiative [26]. Schwartz makes a distinction between the terms "aggregation" and "agglomeration" where "aggregation" denotes delocalization of the π-electrons over adjacent chromophores in the ground state [27] while "agglomeration" denotes polymer chains in close proximity which are not interacting electronically [12]. Aggregation is also used in the literature to describe the configuration of CP chromophores in close proximity where interaction may occur either in the ground state or the excited state [11].

AMPLIFIED FLUORESCENCE QUENCHING/SUPERQUENCHING AND SENSING OPPORTUNITIES

It was soon recognized by Swager et al. that the quenching of conjugated polymer emission arising from exciton diffusion to a small number of defect sites, though a problem in the fabrication of efficient polymer-based LEDs, could be exploited to great advantage in a sensing device. A detection platform with amplified sensitivity to chemical and biological substrates was realized, where the binding of an analyte induced a defect site that would quench the fluorescence of un-doped polymers, or the conductivity of doped polymers. This was called the "molecular wire" effect [28,29] since the amplified sensitivity depended upon the interruption of the wire-like electronic transport along the polymer chain.

A scheme for the detection of small molecules (electron acceptors) exploiting the unique exciton transport properties on a poly(phenylene-ethynylene) conjugated polymer was realized by the design of macrocycles that would bind, as a proof of concept, the methyl viologen dication (MV^{2+}, an excellent electron acceptor) [29]. Exciton transport along the polymer backbone led to the amplification of a fluorescence chemosensory event (binding of MV^{2+}) on what was termed "amplified fluorescence quenching". Comparison of the monomeric macrocycle with its polymeric analogue illustrated the high sensitivity to fluorescence quenching of the latter due to the enhanced transport properties in the polymer, which exhibited a Stern–Volmer fluorescence quenching constant (K_{SV}, see below) 65 times greater than that of the monomer [29].

The sensitivity to fluorescence quenching is typically reported in terms of the slope of a Stern–Volmer plot which correlates the ratio of initial emission intensity over residual intensity (I_0/I) with increasing quencher concentration [Q]. The slope of this plot determines the Stern–Volmer constant, or K_{SV}, defined as the product of the quenching constant k_q and the decay lifetime in the absence of quencher τ_0 (eq. 1). The effect of analytes on K_{SV} can be understood in terms of how they individually affect k_q when dynamic quenching exists. For static quenching, the K_{SV} can be rewritten as an equilibrium constant in as far as the quencher–polymer complex (PQ) is non-emissive (eq. 2). Alterations in the binding equilibrium will therefore also affect the quenching sensitivity and K_{SV}. A large K_{SV} indicates that the conjugated polymer is very sensitive to the increasing quencher concentration [30].

$$\frac{I_0}{I} = 1 + k_q \times \tau_0 \times [Q] = 1 + K_{SV}[Q] \quad (1)$$

$$\frac{I_0 - I}{I} = \frac{[\mathrm{PQ}]}{[\mathrm{P}]} = K_{\mathrm{SV}}[Q] \tag{2}$$

A seminal paper by the Whitten group in 1999 initiated the use of water-soluble CPEs in biosensing. They showed that the anionic PPV derivative MPS-PPV was efficiently quenched by MV^{2+} tethered to a ligand (biotin molecule in this case), and that it exhibited almost complete fluorescence recovery upon addition of avidin, which removed the biotin [31].

The quenching constant of MPS-PPV was compared to that of *trans*-stilbene, whose structure is analogous to the repeating unit in a PPV [31]. While MV^{2+} quenches *trans*-stilbene with a K_{SV} of 15 M^{-1}; the K_{SV} value was 6 orders of magnitude greater for the quenching of MPS-PPV (K_{SV} = 10^7 M^{-1}). This remarkable enhancement in K_{SV} was attributed to the association between the CPE and the quencher driven both by electrostatic and hydrophobic interactions, and by the efficient energy migration along the MPS-PPV backbone. As a consequence of energy migration, excited states formed anywhere along the polymer backbone are quenched by a single MV^{2+} bound anywhere along the polymer chain. The term "superquenching" was coined to reflect the CPE exquisite sensitivity [31,32]. As was later emphasized by Swager [2], much of the quenching amplification in this case resulted from the high fluorophore-quencher binding constant, which must also be taken into account when evaluating the K_{SV} of a conjugated polymer.

CONJUGATED POLYELECTROLYTE–SURFACTANT INTERACTIONS

Shortly after their seminal contribution on the use of MPS-PPV in biosensing, Whitten, Chen, and coworkers first reported on the effects of surfactants on CPEs [33,34]. They noted that MPS-PPV exhibited a 20-fold increase in fluorescence upon addition of the cationic surfactant dodecyltrimethylammonium bromide (DTA) at a surfactant:polymer ratio of 1:3 [33,34]; they additionally noticed a significant blue shift in the emission spectra with increasing surfactant concentration. The increase in intensity was attributed to a restructuring of the conjugated polymer conformation, leading to a reduction in the degree of aggregation and thus hindering the efficiency of through-space energy transfer to non-emissive sites [33–36]. The emission blue shift in turn was attributed to a decrease in the efficiency of through-space energy transfer, resulting in relatively greater emission of higher-energy chromophores in detriment of low-energy sites. The hydrophobicity of the surfactant tails also modified the sensitivity of the MPS-PPV to neutral and cationic quenchers, improving the association of neutral aromatic quenchers such as trinitrotoluene, while hindering the binding of the cationic quencher MV^{2+} which led to a 2 orders-of-magnitude drop in the K_{SV} value for quenching by MV^{2+} [33]. It was shown in subsequent experiments that the K_{SV} values measured were dependent on the structure of the surfactant used: the bilayer-forming surfactant 1,2-dioleoyl-3-trimethylammonium propane (DOTAP) produced only a 2-fold decrease in K_{SV} (5×10^6 M^{-1}) [36].

CONJUGATED POLYELECTROLYTE–LIPID INTERACTIONS

Our work with CPEs was sparked by an interest in generating a technology capable of addressing (via fluorescence) individual surface-tethered liposomes in order to conduct high-throughput membrane binding assays [37–40] on liposome arrays [41]. We have been working on an innovative solution relying on the encapsulation of water-soluble CPEs within liposomes to generate a liposome beacon platform. Our design exploits the efficient exciton migration along CPEs (see above) and the large CPE hydrodynamic radius.

Zwitterionic lipid DOPC

We initially worked on the encapsulation of MPS-PPV within 100-nm-diameter liposomes prepared from the zwitterionic lipid dioleoylphosphatidyl-choline (DOPC) [37]. DOPC lipid films were hydrated with MPS-PPV containing solutions and extruded in order to obtain unilamellar liposomes entrapping MPS-PPV. Quenching studies with MV^{2+} revealed that a fraction of the CPE (ca. 9 %) was entrapped within the liposome and remained inaccessible to MV^{2+} (a charged molecule unable to cross the lipid bilayer), see Fig. 3.

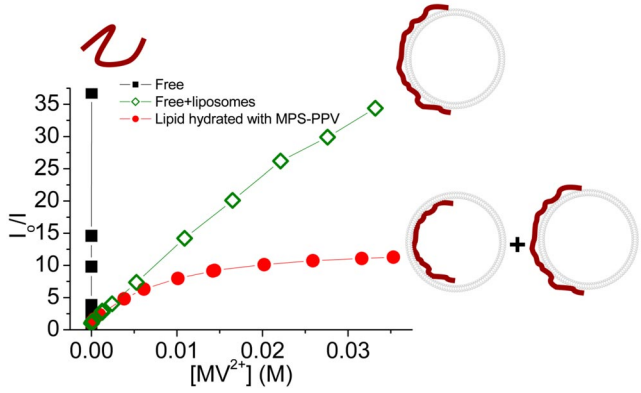

Fig. 3 Fluorescence quenching upon adding increasing $[MV^{2+}]$ to: (■) an MPS-PPV solution 1.6×10^{-5} M in monomer units; (◇) an MPS-PPV solution 1.6×10^{-5} M in monomer units to which a suspension of pre-formed DOPC liposomes (final [DOPC] = 2×10^{-4} M) is initially added; (●) a liposome-encapsulated MPS-PPV solution (DOPC lipid films hydrated with MPS-PPV solutions to yield a final 20 mM DOPC and 1.6 mM MPS-PPV in monomer units solution which is further diluted 100-fold). All experiments are done in 150 mM NaCl and 10 mM HEPES buffer solutions. The lines connecting the experimental points are a visual aid. Modified from ref. [37] with permission from the American Chemical Society.

While we anticipated minimal electrostatic interactions between the negatively charged MPS-PPV and zwitterionic DOPC, hydrophobic interactions led to the complexation of the CPE with DOPC. Thus, in experiments where we mixed preformed liposomes and MPS-PPV we observed a significant blue shift in the emission peak of MPS-PPV and an emission intensity enhancement (a blue shift and intensity enhancement in MPS-PPV emission as a result of surfactant association had been reported by Chen, see the previous section and ref. [33]). Additionally, a 2 orders-of-magnitude drop in the Stern–Volmer quenching constant ($K_{SV} = 1.0 \times 10^3$ M^{-1}) was recorded for the quenching of MPS-PPV by MV^{2+} in the presence of preformed liposomes, with respect to free polymer ($K_{SV} = 1.0 \times 10^5$ M^{-1} under identical ionic strength conditions, see Fig. 3) [37,38]. Subsequent cryo-TEM studies conducted in our group confirmed that MPS-PPV readily interacts with DOPC membranes [39].

Altogether, our results showed that when MPS-PPV is added to solutions containing preformed liposomes, the polymer readily embeds within the membrane (where the hydrophobic polymer backbone presumably lies within the hydrophobic region of the outer leaflet) but remains available to quenching. When lipid films are hydrated with solutions of MPS-PPV, a fraction of the polymer is effectively encapsulated within the liposome, where it presumably binds to the inner membrane leaflet and is thus inaccessible to the quencher MV^{2+} (see Figs. 3 and 4).

The paradigm of CPE–lipid interaction (where the CPE is embedded either within the outer or the inner membrane leaflet according to the preparation methods of the liposomes) provided interesting opportunities to address surface immobilized liposomes. Single-molecule experiments [42–44] conducted in our laboratories on surface-immobilized liposomes prepared according to well-established

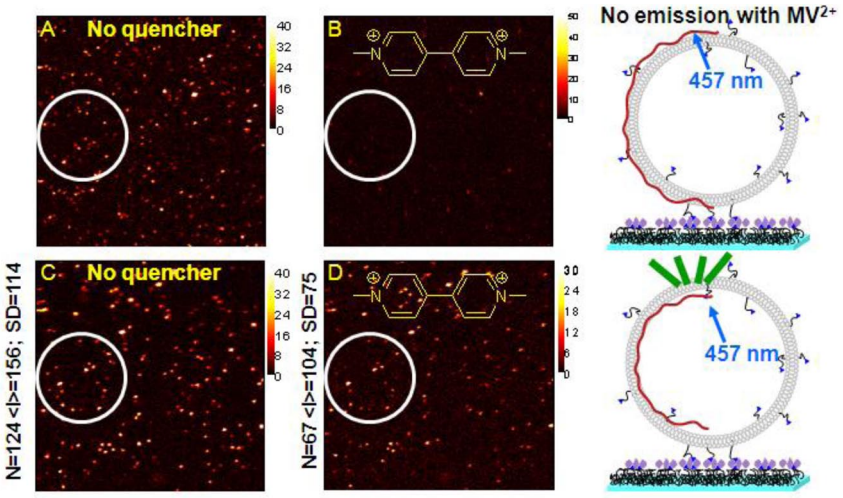

Fig. 4 Fluorescence intensity images obtained before (A and C) and after (B and D) flowing 20 mM MV^{2+} upon 457.9 nm excitation of surface-tethered liposomes containing MPS-PPV. The right bar illustrates the counts per millisecond per pixel. Top panel: preformed liposomes mixed with MPS-PPV. Bottom panel, lipid films hydrated with MPS-PPV solutions to enable CPE encapsulation. The annotations to the left of the bottom panel images indicate the number (*N*) of particles, their average intensity (<*I*>) and the standard deviation (SD) in the <*I*> value. Images are 30 × 30 μm in size. Modified from ref. [37] with permission from the American Chemical Society.

procedures [41,45–47] showed that when MPS-PPV and preformed liposomes were mixed, addition of MV^{2+} quenched the immobilized particle emission (see Fig. 4, top panel), however, when the liposomes were prepared following hydration with MPS-PPV solution (thus favoring the CPE entrapment within the liposome) ca. 50 % of the particles remained emissive. Furthermore, on average the particle intensity for the 50 % emissive population dropped only by 30 % compared to images acquired prior to quencher addition (Fig. 4, bottom panel). We may foresee that liposomes encapsulating CPEs may readily report on membrane permeation (through, e.g., pore-forming proteins or drugs) by a fluorescence-quenching analyte, whereas liposomes embedding CPEs in their outer leaflet will be sensitive to outer membrane leaflet perturbations.

Importantly, the DOPC-CPE interactions dramatically reduced the exciton transport properties along the CPE backbone, as revealed both by the spectroscopic changes described above (intensity enhancement and blue shift in the emission peak) as well as by the drop in K_{SV} values (which drops not only because the membrane prevents the access/reduces the affinity of the quencher for the polymer, but also because exciton transport to the quencher bound site is inefficient). As such, the high sensitivity that characterizes CPEs is significantly compromised, and phenomena such as amplified fluorescence quenching or superquenching may not be observed under these conditions, where the polymer embeds within membranes and is not aggregated.

Zwitterionic lipid DOPC and Ca^{2+}

The dication Ca^{2+} is known to bind to zwitterionic lipids, conferring upon them cationic properties [48–51]). We anticipated that studies with Ca^{2+} would enable us to monitor MPS-PPV response to lipids when both hydrophobic and electrostatic interactions are present. We studied the potential for tuning the polymer properties toward biosensing and energy harvesting under these conditions [38].

A first observation was that Ca^{2+} ions favor the formation of aggregates of the anionic CPE MPS-PPV, as revealed by the lower emission quantum yield and red shift of the emission peak in Ca^{2+}-containing solutions of the CPE. A second observation is that in Ca^{2+}-containing solutions, com-

plexation of lipids with MPS-PPV reaches a plateau upon addition of stoichiometric amounts of lipid molecules to MPS-PPV polymer monomers (see Fig. 5). This was determined from the blue shift in the emission peak and from the emission intensity enhancement for MPS-PPV, and indicated that contrary to Na^+-containing solutions where a large excess of lipid is needed, in Ca^{2+}-containing solutions the electrostatic interactions induced by the dication favor strong binding between the polymer and the zwitterionic lipid DOPC. A third observation was that the order in which lipid solutions and MPS-PPV solutions are mixed plays a key role in determining the spectroscopic properties when the solutions contain Ca^{2+}, see Fig. 5.

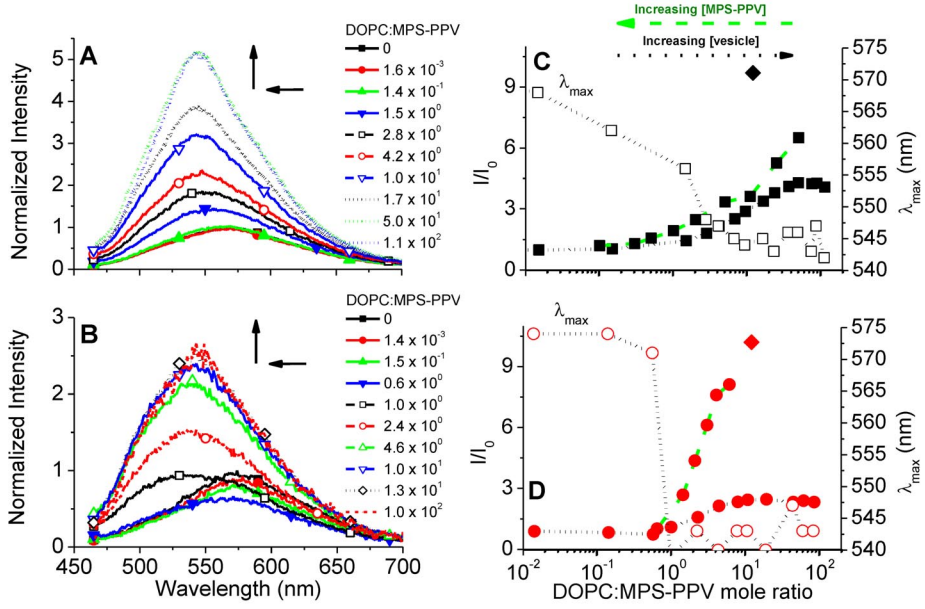

Fig. 5 Titration of MPS-PPV with DOPC vesicles and vice versa: Background-subtracted MPS-PPV emission spectra obtained upon increasing vesicle addition in (A) 30 mM NaCl, 10 mM HEPES, pH 7.2, with 1.5×10^{-5} M MPS-PPV. (B) 10 mM $CaCl_2$, 10 mM HEPES, pH 7.2, with 1.5×10^{-5} M MPS-PPV. Figures A and B were normalized to the emission of free MPS-PPV in Na^+ and Ca^{2+} buffers, respectively. (C) Intensity enhancement (■) and peak shift (□) vs. DOPC:MPS-PPV mol ratio measured in Na^+ buffer. The experimental points correspond to the ratio of intensity at the MPS-PPV emission maximum measured with free polymer i.e., no lipids (I_0) and with increasing lipid concentration (I) for data from (·····) titration of MPS-PPV with DOPC vesicles, (-----) titration of DOPC vesicles with MPS-PPV, (◆) MPS-PPV blended with DOPC at a DOPC:MPS-PPV ratio of 12. (D) Intensity enhancement (●) and peak shift (○) vs. DOPC:MPS-PPV mol ratio measured in Ca^{2+} buffer. The experimental points correspond to (·····) titration of MPS-PPV with DOPC vesicles, (----) titration of DOPC vesicles with MPS-PPV, (◆) MPS-PPV blended with DOPC at a DOPC:MPS-PPV ratio of 12. The lines connecting the experimental points are a visual aid. Reprinted from ref. [38] with permission from the American Chemical Society.

Rapid addition of lipid to polymer yielded large agglomerates that experienced only partial emission intensity enhancement and gave rise to emission spectra showing contributions both from aggregated (red-shifted) and membrane embedded (blue-shifted) MPS-PPV. Under these conditions, a high density of MPS-PPV in lipids was observed where the polymers were trapped in close proximity to each other; as a result the exciton migrated efficiently to non-emissive traps, limiting the MPS-PPV fluorescence enhancement to ca. 2-fold with increasing lipid to polymer monomer ratio. Rapid exciton transport could also be observed when the lipids were enriched with the lipophilic fluorophore 1,1'-dioctadecyl-3,3,3',3'-tetramethylindodicarbocyanine perchlorate (DiD), which can quench MPS-PPV via

Förster resonance energy transfer. At conditions of 5:1500:1500 DiD:DOPC:MPS-PPV monomer units mole ratio, each DiD was able to quench by 50 % the emission of 300 polymer repeat units or 30 MPS-PPV quasi-chromophores, assuming a chromophore length of 10 monomers [52].

We may conclude this section by stating that the interplay of a zwitterionic lipid, the CPE MPS-PPV, divalent cations and buffer provides a rich diversity in architectures and photophysical properties for MPS-PPV.

Anionic lipid DOPA

Our initial studies led us to conclude that zwitterionic lipids mostly interact with MPS-PPV via hydrophobic interactions, and that the addition of Ca^{2+} introduces attractive electrostatic interactions (much like would be expected with cationic lipids) between the negatively charged CPE and the Ca^{2+}-bound lipid. We then searched for conditions that would reduce the overall complexation of MPS-PPV with lipids, i.e., conditions that would minimize the otherwise observed membrane embedding of MPS-PPV. Those conditions would restore the rapid, through-space, energy transfer mechanism, which is a characteristic of free MPS-PPV.

We reasoned that liposomes consisting of negatively charged lipids should show little if any complexation with the negatively charged polymer MPS-PPV. We thus sought for the encapsulation of MPS-PPV within 200 nm liposomes consisting of 75 % dioleoylphosphatidic acid (DOPA) and 25 % DOPC. A series of ensemble spectroscopic studies, gel filtration chromatography combined with fluorescence studies, cryo-TEM imaging studies on vitrified samples containing MPS-PPV only, as well as MPS-PPV encapsulated within DOPC and DOPA liposomes under two lipid:MPS-PPV monomer ratios (20:1 and 1:1); together with single-molecule spectroscopy studies (see below) enabled us to conclude that MPS-PPV is encapsulated within the 3:1 DOPA:DOPC liposomes yet freely diffusing within them, i.e., it does not embed in the membrane [39].

The ability to entrap freely diffusing MPS-PPV single molecules within 200-nm liposomes provided a system to study CPE photophysics in solution at the single-molecule level for extended periods of time upon liposome surface immobilization. A molecular-level visualization of vesicles and of MPS-PPV via cryo-TEM, combined with our single-molecule spectroscopy results on MPS-PPV, in turn enabled us to directly correlate for the first time the CPE conformation with its spectroscopic features. We observed densely packed MPS-PPV aggregates in vitrified samples containing polymer only. In the case of samples prepared with 3:1 DOPA:DOPC and MPS-PPV, whereas we were unable to unequivocally distinguish polymer particles from ice contamination, we certainly observed that the liposomes were predominantly unilamellar irrespective of the lipid:MPS-PPV monomer mole ratio explored, presumably, MPS-PPV is also densely packed/aggregated under these conditions. In marked contrast, images of vitrified samples containing liposomes prepared with DOPC hydrated with MPS-PPV showed multilamellar liposomes, even at 20:1 DOPC:MPS-PPV monomer mol ratios, but notably at 1:1 DOPC:MPS-PPV monomer mole ratios. The binding of multiple bilayers is mediated by MPS-PPV.

Single-molecule spectroscopy studies (see Fig. 6) on surface-immobilized liposomes containing a single MPS-PPV polymer molecule were greatly informative. We found that in DOPC liposomes, the CPE emission intensity decayed in an exponential manner with time following photobleaching, and that the polymer single-molecule emission spectra were significantly blue shifted and identical to the ensemble emission spectrum for MPS-PPV embedded within DOPC membranes. Both results are in line with the hypothesis that the MPS-PPV polymer molecule consists of a large number of independent chromophores when embedded in DOPC, emission arises from each and all of them, and complete photobleaching requires the suppression of emission from all these chromophores. In marked contrast, the intensity-time trajectories obtained via single-molecule spectroscopy studies of 3:1 DOPA:DOPC liposomes encapsulating MPS-PPV showed single-step (on occasions, reversible) photobleaching. The emission spectra for the single polymer molecules were centered at ca. 560 nm. Combined, the single-step photobleaching and single-molecule emission spectra indicate that a few low-energy emissive sites

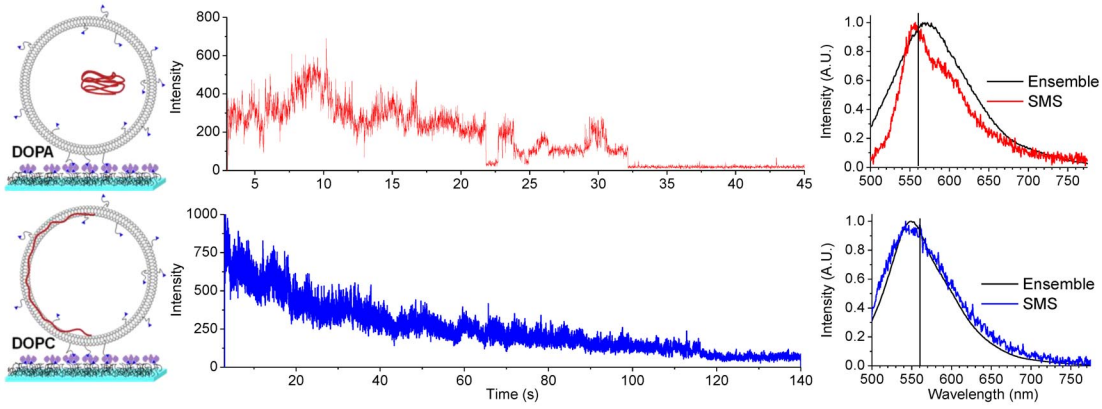

Fig. 6 Left: Cartoon illustrating the encapsulated polymer, middle: intensity-time trajectories for MPS-PPV, acquired upon 514 nm excitation of MPS-PPV encapsulated in vesicles containing no DiD (10 ms dwell time). Right: Single-molecule emission spectra for MPS-PPV. Top panel: Anionic vesicles (DOPA:DOPC; 3:1). Bottom panel: Neutral vesicles (DOPC). The single-molecule emission spectra for MPS-PPV were obtained upon 488 nm excitation and using a 500-nm-long pass filter. Overlaid to these spectra (black traces) are ensemble steady-state emission spectra acquired for the same samples. Reprinted from ref. [39] with permission from the National Academy of Sciences, USA.

(chromophores) exist within the polymer backbone when MPS-PPV is freely diffusing and that energy is efficiently funneled to these sites [20,22,53].

New to this work was the ability to study the spectroscopy of single, freely diffusing polymers (albeit confined in vesicles) while controlling the polymer–matrix interaction by tuning the membrane charge. The molecular visualization from cryo-TEM studies enabled us to ultimately assign a polymer conformation to its unique photophysics.

Other recent studies on polymer–lipid interactions

Recently, the complexation of CPEs with phospholipids and the changes they impart to the polymer emission properties have been exploited in novel lipase-sensing platforms [54,55], sensor arrays for detection, and differentiation of different cell lines [56] as well as novel biocidal agents [54,57,58]. The interplay of electrostatic and hydrophobic interactions between the CPEs and lipids is crucial to the success of these devices. For example: (i) The transformation of zwitterionic phosphocholine lipids into negatively charged phosphatidic acids by lipases upon hydrolysis of the phosphoester bond reduces lipid–polymer interactions and renders polymers non-emissive. Schanze et al. exploited the surfactant-induced enhancement of CPE fluorescence to create a biosensor for lipase activity. The association of 0–15 μM zwitterionic phospholipids with a 1-μM solution of the anionic poly(phenylene ethynylene) $BpPPESO_3$ produces a blue shift of up to 67 nm and a fluorescence enhancement of up to 50-fold; such effects are reversed upon hydrolysis of the phospholipid by the enzyme phospholipase C [55]. (ii) The desorption of negatively charged CPEs from a positively charged fluorescence-quenching Au nanoparticle scaffold upon interaction with the membranes of cells enables the specific detection of cancer cells [56]. (iii) The specific polyelectrolyte–lipid interaction enables in situ singlet oxygen sensitization on the cellular membrane of bacteria [54,57,58]. The above studies are the first examples where conjugated polyelectrolyte–lipid interactions and their effect on the CPE spectroscopic behavior are exploited in devices with biological applications.

CONCLUSIONS

Understanding and controlling the extent of energy transfer along the polymer backbone is critical to the exploitation of CPEs in biosensing platforms. Motivated by our interest in developing a "liposome beacon platform", we have conducted both ensemble and single-molecule spectroscopic studies on the interaction of the CPE MPS-PPV with anionic, neutral, and positively charged (via Ca^{2+} complexation) lipids. The diversity of the resulting architectures as well as their unique spectroscopic characteristics provide for a wide range of opportunities toward developing hybrid lipid-conjugated polymer/polyelectrolyte optoelectronic devices. We may mention the good light-harvesting properties encountered in agglomerates of MPS-PPV and lipids in the presence of Ca^{2+}, where the polymer remains highly aggregated and where the membrane provides for a suitable interface to accommodate, e.g., light-harvesting materials. We may quote the outstanding intensity enhancements observed following MPS-PPV embedding within zwitterionic membranes, a result of the deaggregation of the polymer chains. The membrane-mediated deaggregation yields a very emissive material on a highly malleable membrane scaffold. We may also cite the poor complexation of CPEs and lipids of equal charge, e.g., DOPA and MPS-PPV, both negatively charged species, which ensures that the CPE retains its efficient through-space energy transport properties, characterized by a low emission yield. These unique properties and the ability to tune them surely are appealing in devising enzyme sensors. Lipase sensing schemes have already exploited the changes in the CPE emission quantum yield with membrane charge. Whereas significant progress will undoubtedly occur in the next few years, a major focus should be placed on minimizing conjugated polymer photodegradation.

ACKNOWLEDGMENTS

G.C. is grateful to the Natural Sciences and Engineering Research Council and the Canadian Foundation for Innovation New Opportunities Fund for financial assistance. A.T.N. and P.K. are also thankful to the McGill Chemical Biology Fellowship Program (CIHR) for postgraduate scholarships. A.T.N. is also thankful to the Fonds Québécois de la Recherche sur la Nature et les Technologies (FQRNT) for a postgraduate scholarship.

REFERENCES

1. H. Jiang, P. Taranekar, J. R. Reynolds, K. S. Schanze. *Angew. Chem., Int. Ed.* **48**, 4300 (2009).
2. S. W. Thomas, G. D. Joly, T. M. Swager. *Chem. Rev.* **107**, 1339 (2007).
3. J. R. Reynolds, T. A. Skotheim. *Conjugated Polymers: Theory, Synthesis, Properties, and Characterization*, CRC, Boca Raton (2007).
4. G. D. Scholes, G. Rumbles. *Nat. Mater.* **5**, 683 (2006).
5. J. H. Burroughes, D. D. C. Bradley, A. R. Brown, R. N. Marks, K. Mackay, R. H. Friend, P. L. Burns, A. B. Holmes. *Nature* **347**, 539 (1990).
6. P. S. Vincett, W. A. Barlow, R. A. Hann, G. G. Roberts. *Thin Solid Films* **94**, 171 (1982).
7. A. Kraft, A. C. Grimsdale, A. B. Holmes. *Angew. Chem., Int. Ed.* **37**, 402 (1998).
8. A. C. Grimsdale, A. B. Holmes. In *Conjugated Polymers: Theory, Synthesis, Properties, and Characterization*, J. R. Reynolds, T. A. Skotheim (Eds.), CRC, Boca Raton (2007).
9. A. O. Patil, Y. Ikenoue, F. Wudl, A. J. Heeger. *J. Am. Chem. Soc.* **109**, 1858 (1987).
10. S. Shi, F. Wudl. *Macromolecules* **23**, 2119 (1990).
11. K. S. Schanze, X. Zhao. *Conjugated Polymers: Theory, Synthesis, Properties, and Characterization*, CRC, Boca Raton (2007).
12. B. J. Schwartz. *Annu. Rev. Phys. Chem.* **54**, 141 (2003).
13. C. Tan, E. Atas, J. G. Muller, M. R. Pinto, V. D. Kleiman, K. S. Schanze. *J. Am. Chem. Soc.* **126**, 13685 (2004).

14. G. D. Scholes. *Annu. Rev. Phys. Chem.* **54**, 57 (2003).
15. E. Hennebicq, G. Pourtois, G. D. Scholes, L. M. Herz, D. M. Russell, C. Silva, S. Setayesh, A. C. Grimsdale, K. Müllen, J.-L. Brédas, D. Beljonne. *J. Am. Chem. Soc.* **127**, 4744 (2005).
16. D. Beljonne, G. Pourtois, C. Silva, E. Hennebicq, L. M. Herz, R. H. Friend, G. D. Scholes, S. Setayesh, K. Mullen, J. L. Bredas. *Proc. Natl. Acad. Sci. USA* **99**, 10982 (2002).
17. T.-Q. Nguyen, J. Wu, V. Doan, B. J. Schwartz, S. H. Tolbert. *Science* **288**, 652 (2000).
18. D. A. V. Bout, W.-T. Yip, D. Hu, D.-K. Fu, T. M. Swager, P. F. Barbara. *Science* **277**, 1074 (1997).
19. A. J. Epstein, J. W. Blatchford, Y. Z. Wang, S. W. Jessen, D. D. Gebler, T. L. Gustafson, L. B. Lin, H. L. Wang, Y. W. Park, T. M. Swager, A. G. MacDiarmid. *Synth. Met.* **78**, 253 (1996).
20. J. Yu, D. Hu, P. F. Barbara. *Science* **289**, 1327 (2000).
21. H. Bässler, B. Schweitzer. *Acc. Chem. Res.* **32**, 173 (1999).
22. T. Huser, M. Yan, L. J. Rothberg. *Proc. Natl. Acad. Sci. USA* **97**, 11187 (2000).
23. T. E. Dykstra, E. Hennebicq, D. Beljonne, J. Gierschner, G. Claudio, E. R. Bittner, J. Knoester, G. D. Scholes. *J. Phys. Chem. B* **113**, 656 (2009).
24. T. M. Swager, C. J. Gil, M. S. Wrighton. *J. Phys. Chem.* **99**, 4886 (1995).
25. R. D. Scurlock, B. Wang, P. R. Ogilby, J. R. Sheats, R. L. Clough. *J. Am. Chem. Soc.* **117**, 10194 (1995).
26. C. J. Collison, L. J. Rothberg, V. Treemaneekarn, Y. Li. *Macromolecules* **34**, 2346 (2001).
27. U. Lemmer, S. Heun, R. F. Mahrt, U. Scherf, M. Hopmeier, U. Siegner, E. O. Goebel, K. Muellen, H. Baessler. *Chem. Phys. Lett.* **240**, 373 (1995).
28. T. M. Swager. *Acc. Chem. Res.* **31**, 201 (1998).
29. Q. Zhou, T. M. Swager. *J. Am. Chem. Soc.* **117**, 7017 (1995).
30. J. R. Lakowicz. *Principles of Fluorescence Spectroscopy*, Springer, New York (2006).
31. L. Chen, D. W. McBranch, H.-L. Wang, R. Helgeson, F. Wudl, D. G. Whitten. *Proc. Natl. Acad. Sci. USA* **96**, 12287 (1999).
32. K. E. Achyuthan, T. S. Bergstedt, L. Chen, R. M. Jones, S. Kumaraswamy, S. A. Kushon, K. D. Ley, L. Lu, D. McBranch, H. Mukundan, F. Rininsland, X. Shi, W. Xia, D. G. Whitten. *J. Mater. Chem.* **15**, 2648 (2005).
33. L. Chen, S. Xu, D. McBranch, D. Whitten. *J. Am. Chem. Soc.* **122**, 9302 (2000).
34. L. Chen, D. McBranch, R. Wang, D. Whitten. *Chem. Phys. Lett.* **330**, 27 (2000).
35. J. S. Treger, V. Y. Ma, Y. Gao, C.-C. Wang, H.-L. Wang, M. S. Johal. *J. Phys. Chem. B* **112**, 760 (2008).
36. J. Dalvi-Malhotra, L. Chen. *J. Phys. Chem. B* **109**, 3873 (2005).
37. A. T. Ngo, P. Karam, E. Fuller, M. Burger, G. Cosa. *J. Am. Chem. Soc.* **130**, 457 (2008).
38. A. T. Ngo, G. Cosa. *Langmuir* **26**, 6746 (2010).
39. P. Karam, A. T. Ngo, I. Rouiller, G. Cosa. *Proc. Natl. Acad. Sci. USA* **107**, 17480 (2010).
40. A. T. Ngo, K. L. Lau, J. Quesnel, R. Aboukhalil, G. Cosa. *Can. J. Chem.* (2011). In press.
41. S. M. Christensen, D. Stamou. *Soft Matter* **3**, 828 (2007).
42. W. E. Moerner, M. Orrit. *Science* **283**, 1670 (1999).
43. S. Nie, R. Zare. *Annu. Rev. Biophys. Biomol. Struct.* **26**, 567 (1997).
44. X. S. Xie, J. K. Trautman. *Annu. Rev. Phys. Chem.* **49**, 441 (1998).
45. E. Boukobza, A. Sonnenfeld, G. Haran. *J. Phys. Chem. B* **105**, 12165 (2001).
46. I. Cisse, B. Okumus, C. Joo, T. Ha. *Proc. Natl. Acad. Sci. USA* **104**, 12646 (2007).
47. D. Stamou, C. Duschl, E. Delamarche, H. Vogel. *Angew. Chem., Int. Ed.* **42**, 5580 (2003).
48. D. P. Kharakoz, R. S. Khusainova, A. V. Gorelov, K. A. Dawson. *FEBS Lett.* **446**, 27 (1999).
49. J. Marra, J. Israelachvili. *Biochemistry* **24**, 4608 (1985).
50. L. J. Lis, W. T. Lis, V. A. Parsegian, R. P. Rand. *Biochemistry* **20**, 1771 (1981).
51. J. J. McManus, J. O. Raedler, K. A. Dawson. *J. Phys. Chem. B* **107**, 9869 (2003).
52. H. S. Woo, O. Lhost, S. C. Graham, D. D. C. Bradley, R. H. Friend, C. Quattrocchi, J. L. Brédas, R. Schenk, K. Müllen. *Synth. Met.* **59**, 13 (1993).

53. D. H. Hu, J. Yu, K. Wong, B. Bagchi, P. J. Rossky, P. F. Barbara. *Nature* **405**, 1030 (2000).
54. S. Chemburu, E. Ji, Y. Casana, Y. Wu, T. Buranda, K. S. Schanze, G. P. Lopez, D. G. Whitten. *J. Phys. Chem. B* **112**, 14492 (2008).
55. Y. Liu, K. Ogawa, K. S. Schanze. *Anal. Chem.* **80**, 150 (2008).
56. A. Bajaj, O. R. Miranda, I.-B. Kim, R. L. Phillips, D. J. Jerry, U. H. F. Bunz, V. M. Rotello. *Proc. Natl. Acad. Sci. USA* **106**, 10912 (2009).
57. T. S. Corbitt, J. R. Sommer, S. Chemburu, K. Ogawa, L. K. Ista, G. P. Lopez, D. G. Whitten, K. S. Schanze. *ACS Appl. Mater. Interfaces* **1**, 48 (2008).
58. L. Ding, E. Y. Chi, S. Chemburu, E. Ji, K. S. Schanze, G. P. Lopez, D. G. Whitten. *Langmuir* **26**, 5544 (2010).

